


Calculation of the wake due to radiation and space charge forces in relativistic beams

Gennady Stupakov[✉] and Jingyi Tang[✉]

SLAC National Accelerator Laboratory, Menlo Park 94025, California, USA

 (Received 25 June 2020; accepted 19 January 2021; published 4 February 2021)

Radiation reaction force in a relativistic beam, also known as the CSR wakefield, is often computed using a 1D model of a line charge. While this model can serve as a useful tool for a quick calculation, in many cases its accuracy is not sufficient. In particular, this model misses the so-called compression effects associated with the change of the electromagnetic energy when the beam is compressed longitudinally or transversely. The existing 3D simulation codes that take this effect into account are often slow and are not easy to use. In this work, we propose a new approach to the calculations of radiation and space charge longitudinal forces in free space based on the use of the integrals for the retarded potentials. Our main result expresses the rate of change of particles' energy through 2D (in a 2D model) or 3D integrals along the beam orbit.

DOI: [10.1103/PhysRevAccelBeams.24.020701](https://doi.org/10.1103/PhysRevAccelBeams.24.020701)

I. INTRODUCTION

When the trajectory of a relativistic beam is bent by magnetic field, the beam radiates electromagnetic field and experiences a radiation reaction force. This force plays an important role in generation, transport and accumulation of high-current, low-emittance electron beams, and is customarily designated as the coherent synchrotron radiation (CSR) wakefield. Its account is crucial in the design of bunch compressors for modern x-ray free electron lasers (FELs) and linear colliders. It can also affect the beam dynamics in electron synchrotron accelerators.

There are several approaches to the calculation of the CSR wakefield. A popular 1D model for a circular motion in free space was developed in Refs. [1–3]. It has later been generalized in Refs. [4,5] for a bending magnet of finite length and is currently implemented in several computer codes routinely used for simulations of beam dynamics in accelerators. Various refinements and improvements of the original 1D model, as well as generalization for a beam line with several bending magnets, can be found in Refs. [6–9].

The CSR wake in free space is often a good approximation to reality for extremely short bunches encountered in bunch compressors of FELs, where the bunch length after compression can be as small as tens of microns. In electron synchrotrons, where the typical bunch length is in the range of centimeters, the metal boundaries of the

vacuum chamber cannot be neglected. These boundaries introduce the so-called shielding effect that suppresses both the synchrotron radiation at low frequencies and the CSR wake, often to the level when it can be neglected. Various aspects of the shielding effect are studied in Refs. [6,10–18]. In this paper, we ignore the shielding effect of the metal boundaries aiming our study to the very short bunches of modern linear accelerator.

The 1D models mentioned above are simple and easy to use but they might miss an important part of the total force in relativistic beams moving in a curvilinear trajectory. The attention to this force was attracted by M. Dohlus in 2002 [19], when he pointed out that if the beam is compressed (either longitudinally or transversely) the change of the energy of its Coulomb field alters the kinetic energy of the beam particles. A force that is responsible for this change can be called the compression force. Note that this force is different from the radiation reaction force because the compression is a reversible process—this force changes sign when the beam is being decompressed. It cannot be associated with what is conventionally called the *space charge force* because the latter typically scales as γ^{-2} with γ the Lorentz factor. The compression-decompression effect occurs even in the limit $\gamma \rightarrow \infty$ (hence, $v = c$), when the conventional space charge force vanishes.

The 3D approach to the calculation of the CSR wake in free space is often based on the Liénard-Wiechert expressions for the electromagnetic field of a point charge [20–22]. One of the difficulties of this approach is that even at finite distance from the radiating particle there are spatial regions where its field varies on extremely small scale $\propto \gamma^{-3}$. In the ultrarelativistic limit, $\gamma \rightarrow \infty$, the field has a singularity line [20] which requires a special treatment.

Published by the American Physical Society under the terms of the [Creative Commons Attribution 4.0 International license](https://creativecommons.org/licenses/by/4.0/). Further distribution of this work must maintain attribution to the author(s) and the published article's title, journal citation, and DOI.

Currently the model developed in Refs. [21,22] is still limited to a steady state wake of a bunch moving on a circular orbit. This difficulty is overcome in the 3D option of the computer program CSRTRACK [23] through the introduction of a pseudo-Green function of a spherically symmetric macroparticles in the beam. Unfortunately, CSRTRACK requires a large number of macro particles and long run time to calculate the wake for practical beam lines.

In this paper we propose a different approach to the calculation of the 3D CSR wake when the beam propagates in free space (that is neglecting the effects of metal boundaries). In our approach, the beam is represented by its charge density $\rho(\mathbf{r}, t)$ that depends on time t and coordinate vector \mathbf{r} , and its velocity $\mathbf{v}(\mathbf{r}, t)$, with the beam current density \mathbf{j} given by the product $\mathbf{j} = \rho\mathbf{v}$. For given functions $\rho(\mathbf{r}, t)$ and $\mathbf{j}(\mathbf{r}, t)$ we then derive an equation for the electric field in the beam, $\mathbf{E}(\mathbf{r}, t)$, and calculate the instantaneous energy change per unit time and *per unit charge*,

$$\mathcal{W}(\mathbf{r}, t) = \mathbf{v}(\mathbf{r}, t) \cdot \mathbf{E}(\mathbf{r}, t). \quad (1)$$

The result is expressed as an integral over the volume around the beam trajectory at preceding times, $t_{\text{ret}} < t$. We will loosely call \mathcal{W} the *longitudinal wake*, even though the classical wakefields are typically associated with the energy loss integrated over the transverse cross section of the beam.

A similar approach to the calculation of electromagnetic fields was advocated in Refs. [17,18], although the emphasis in those papers was on the proper account of the metal boundaries and the effects of the wake on particle motion. While the method developed in those papers is adequate for studies of such problems as microbunching instability, where the self-consistent nature of the particle-field interaction is crucial, here we aim at the applications of the CSR wake in situations when it is relatively small and can be treated as a perturbation. These situations appear in the design of bunch compressors with a high peak current where even a relatively small CSR wake can lead to a large transverse emittance growth of the beam.

An initial part of this work has been started by one of the authors (GS) in collaboration with D. Ratner and is documented in D. Ratner's thesis [24]. Preliminary results of our study have been reported in Refs. [25–27]—for completeness we included some of them in this paper.

This paper is organized as follows. In Sec. II we derive equations for the wakefield \mathcal{W} in terms of a three-dimensional integral along the beam orbit. In Sec. III we specialize these equations for the case of a 2D Gaussian bunch assuming that its trajectory can be described by linear optics. In Sec. IV, the geometrical aspect of the integration in the curvilinear coordinate system associated with the reference orbit of the beam is worked out. In Sec. V a numerical example is presented of the CSR

wakefield of a beam that is being longitudinally compressed inside a bending magnet, and the wakefield is compared with the result of 1D wake and CSRTRACK. In Sec. VI we apply the technique developed in this paper to a bunch compressor and compare the emittance growth in our model with the one calculated for 1D CSR wake. We conclude the paper with Sec. VII by summarizing our results.

We use the CGS system of units throughout this paper.

II. ELECTROMAGNETIC FIELD OF THE BEAM

We start from the so called *retarded potentials* [28]—the expressions for the scalar potential ϕ and the vector potential \mathbf{A} generated by a beam with the charge density ρ and current density $\mathbf{j} = \rho\mathbf{v}$,

$$\begin{aligned} \phi(\mathbf{r}, t) &= \int d^3 r' \frac{\rho(\mathbf{r}', t_{\text{ret}})}{|\mathbf{r}' - \mathbf{r}|}, \\ \mathbf{A}(\mathbf{r}, t) &= \frac{1}{c} \int d^3 r' \frac{\mathbf{v}(\mathbf{r}', t_{\text{ret}})\rho(\mathbf{r}', t_{\text{ret}})}{|\mathbf{r}' - \mathbf{r}|}, \end{aligned} \quad (2)$$

where the retarded time is $t_{\text{ret}}(\mathbf{r}, \mathbf{r}', t) = t - |\mathbf{r}' - \mathbf{r}|/c$ and the integration goes over the whole space. The electric field is given by

$$\mathbf{E}(\mathbf{r}, t) = -\nabla_r \phi(\mathbf{r}, t) - \frac{1}{c} \frac{\partial \mathbf{A}(\mathbf{r}, t)}{\partial t}. \quad (3)$$

To find the contribution to \mathbf{E} from the scalar potential, we evaluate

$$\begin{aligned} \nabla_r \phi &= \int d^3 r' \left(\frac{\nabla_r \rho(\mathbf{r}', t_{\text{ret}})}{|\mathbf{r}' - \mathbf{r}|} + \rho(\mathbf{r}', t_{\text{ret}}) \nabla_r \frac{1}{|\mathbf{r}' - \mathbf{r}|} \right) \\ &= \int d^3 r' \left(\frac{\nabla_r \rho(\mathbf{r}', t_{\text{ret}})}{|\mathbf{r}' - \mathbf{r}|} - \rho(\mathbf{r}', t_{\text{ret}}) \nabla_{r'} \frac{1}{|\mathbf{r}' - \mathbf{r}|} \right), \end{aligned} \quad (4)$$

where we have replaced the gradient ∇_r acting on the variable \mathbf{r} by the gradient $-\nabla_{r'}$ acting on \mathbf{r}' when applied to the combination $|\mathbf{r}' - \mathbf{r}|^{-1}$. Integrating this expression by parts and using the fact that the charge density vanishes at infinity gives

$$\begin{aligned} \nabla_r \phi &= \int \frac{d^3 r'}{|\mathbf{r}' - \mathbf{r}|} [\nabla_r \rho(\mathbf{r}', t_{\text{ret}}) + \nabla_{r'} \rho(\mathbf{r}', t_{\text{ret}})] \\ &= \int \frac{d^3 r'}{|\mathbf{r}' - \mathbf{r}|} \left[\frac{\partial \rho(\mathbf{r}', t_{\text{ret}})}{\partial t_{\text{ret}}} \nabla_r t_{\text{ret}} + \partial_{r'} \rho(\mathbf{r}', t_{\text{ret}}) \right. \\ &\quad \left. + \frac{\partial \rho(\mathbf{r}', t_{\text{ret}})}{\partial t_{\text{ret}}} \nabla_{r'} t_{\text{ret}} \right], \end{aligned} \quad (5)$$

where here (and below) we use the notation $\partial_{r'} \rho(\mathbf{r}', t_{\text{ret}})$ to indicate differentiation with respect to the space coordinates in function $\rho(\mathbf{r}', t_{\text{ret}})$ keeping t_{ret} fixed (in other words,

in contrast to $\nabla_{r'}$, the operator $\partial_{r'}$ ignores the fact that t_{ret} also depends on r' . Noting that $\nabla_{r',t_{\text{ret}}} = -\nabla_{r',t_{\text{ret}}}$, we obtain

$$\nabla_r \phi = \int \frac{d^3 r'}{|\mathbf{r}' - \mathbf{r}|} \partial_{r'} \rho(\mathbf{r}', t_{\text{ret}}). \quad (6)$$

For the contribution to \mathbf{E} from the vector potential we need to calculate the time derivative of \mathbf{A} ,

$$\begin{aligned} \frac{\partial \mathbf{A}}{\partial t} &= \frac{1}{c} \int \frac{d^3 r'}{|\mathbf{r}' - \mathbf{r}|} [\mathbf{v}(\mathbf{r}', t_{\text{ret}}) \partial_{t_{\text{ret}}} \rho(\mathbf{r}', t_{\text{ret}}) \\ &+ \rho(\mathbf{r}', t_{\text{ret}}) \partial_{t_{\text{ret}}} \mathbf{v}(\mathbf{r}', t_{\text{ret}})], \end{aligned} \quad (7)$$

where we have used the fact that $\partial_t = \partial_{t_{\text{ret}}}$. We now use the continuity equation $\partial_t \rho + \nabla \cdot (\rho \mathbf{v}) = 0$ to find $\partial_{t_{\text{ret}}} \rho$,

$$\begin{aligned} \partial_{t_{\text{ret}}} \rho(\mathbf{r}', t_{\text{ret}}) &= -\partial_{r'} \cdot [\mathbf{v}(\mathbf{r}', t_{\text{ret}}) \rho(\mathbf{r}', t_{\text{ret}})] \\ &= -\mathbf{v}(\mathbf{r}', t_{\text{ret}}) \cdot \partial_{r'} \rho(\mathbf{r}', t_{\text{ret}}) \\ &\quad - \rho(\mathbf{r}', t_{\text{ret}}) \partial_{r'} \cdot \mathbf{v}(\mathbf{r}', t_{\text{ret}}). \end{aligned} \quad (8)$$

Putting this expression into Eq. (7) gives

$$\begin{aligned} \frac{\partial \mathbf{A}}{\partial t} &= -\frac{1}{c} \int \frac{d^3 r'}{|\mathbf{r}' - \mathbf{r}|} \mathbf{v}(\mathbf{r}', t_{\text{ret}}) [\mathbf{v}(\mathbf{r}', t_{\text{ret}}) \cdot \partial_{r'} \rho(\mathbf{r}', t_{\text{ret}}) \\ &+ \rho(\mathbf{r}', t_{\text{ret}}) \partial_{r'} \cdot \mathbf{v}(\mathbf{r}', t_{\text{ret}})] \\ &+ \frac{1}{c} \int \frac{d^3 r'}{|\mathbf{r}' - \mathbf{r}|} \rho(\mathbf{r}', t_{\text{ret}}) \partial_{t_{\text{ret}}} \mathbf{v}(\mathbf{r}', t_{\text{ret}}). \end{aligned} \quad (9)$$

Finally, combining Eqs. (6) and (9) we obtain the following expression for $\mathcal{W}(\mathbf{r}, t) = \mathbf{v}(\mathbf{r}, t) \cdot \mathbf{E}(\mathbf{r}, t)$,

$$\mathcal{W} = \mathcal{W}_1 + \mathcal{W}_2 + \mathcal{W}_3, \quad (10)$$

where

$$\begin{aligned} \mathcal{W}_1(\mathbf{r}, t) &= -c \int \frac{d^3 r'}{|\mathbf{r}' - \mathbf{r}|} [\boldsymbol{\beta}(\mathbf{r}, t) - (\boldsymbol{\beta}(\mathbf{r}, t) \cdot \boldsymbol{\beta}(\mathbf{r}', t_{\text{ret}})) \\ &\quad \times \boldsymbol{\beta}(\mathbf{r}', t_{\text{ret}})] \cdot \partial_{r'} \rho(\mathbf{r}', t_{\text{ret}}), \end{aligned} \quad (11a)$$

$$\begin{aligned} \mathcal{W}_2(\mathbf{r}, t) &= c \int \frac{d^3 r'}{|\mathbf{r}' - \mathbf{r}|} (\boldsymbol{\beta}(\mathbf{r}, t) \cdot \boldsymbol{\beta}(\mathbf{r}', t_{\text{ret}})) \rho(\mathbf{r}', t_{\text{ret}}) \\ &\quad \times \partial_{r'} \cdot \boldsymbol{\beta}(\mathbf{r}', t_{\text{ret}}), \end{aligned} \quad (11b)$$

$$\mathcal{W}_3(\mathbf{r}, t) = - \int \frac{d^3 r'}{|\mathbf{r}' - \mathbf{r}|} \rho(\mathbf{r}', t_{\text{ret}}) \boldsymbol{\beta}(\mathbf{r}, t) \cdot \partial_{t_{\text{ret}}} \boldsymbol{\beta}(\mathbf{r}', t_{\text{ret}}), \quad (11c)$$

with $\boldsymbol{\beta} = \mathbf{v}/c$. Note that due to the factor $|\mathbf{r}' - \mathbf{r}|^{-1}$ the integrands have a singularity at $\mathbf{r}' \rightarrow \mathbf{r}$ which, however, is integrable in three dimensions.

Our result Eqs. (11) to some degree is similar to Jefimenko's expression for the electric field of arbitrary charge distribution varying with time [29]. In contrast to Jefimenko's formula, however, we expressed the current density as a product of the charge density and the local velocity in the beam, and eliminated the time derivative of the charge using the continuity equation.

At a first glance, it might seem that \mathcal{W}_2 and \mathcal{W}_3 in Eqs. (11) are much smaller than \mathcal{W}_1 . Indeed, \mathcal{W}_1 involves the spatial derivative of ρ that can be estimated as $|\partial_{r'} \rho| \sim \rho/\sigma$, where σ is the characteristic size of the beam. In the last two integrals, we have the spatial and time derivatives of the velocity field in the beam that are estimated as $|\partial_{r'} \cdot \boldsymbol{\beta}| \sim 1/L$ and $|\partial_{t_{\text{ret}}} \boldsymbol{\beta}| \sim c/L$, respectively, with L the external scale of the problem determined by the magnetic lattice (L can, for example, be associated with the radius of curvature of the beam orbit). If we assume that the size of the beam is much smaller than L , $\sigma \ll L$, it seems that the last two integrals in Eq. (11) would be much smaller than the first one. This conclusion however is not generally true even in the limit $\sigma \ll L$ because the spatial derivative of the distribution, $\partial_{r'} \rho$, changes sign when integrated over the space, and the contributions from various parts of this derivative partially cancel each other, while the integrands in \mathcal{W}_2 and \mathcal{W}_3 involve ρ that is always positive.

The integrals (11) can also be computed in two dimensions with the three dimensional integration $\int d^3 r'$ replaced by a 2D one, $\int d^2 r'$. This corresponds to the model of a ribbon beam where ρ has a meaning of the charge per unit area. Note that the singularity $|\mathbf{r}' - \mathbf{r}|^{-1}$ is still integrable in 2D (however it is not integrable in one dimension of a line charge model). The 2D model of the beam makes sense in bunch compressors where the beam is mostly spread out in the horizontal plane due to the combination of a large dispersion and an energy chirp in the beam. In the rest of this paper we will adopt a 2D version of Eq. (11) which simplifies numerical calculation of the integrals.

We will also make one more approximation assuming a relativistic beam with $\beta = 1$. This assumption eliminates the conventional space charge forces that scale as γ^{-2} . Note that in this limit the singularity $|\mathbf{r}' - \mathbf{r}|^{-1}$ in the integrand of Eq. (11a) disappears because the expression in the square brackets tends to zero when $\mathbf{r}' \rightarrow \mathbf{r}$.

Finally, we note that in principle Eqs. (11) can be generalized to include the shielding effect of metal parallel plates using image charges, as it has been done in Refs. [6,16].

III. GAUSSIAN BEAMS AND BEAM OPTICS

The CSR wake alters particles' energy, modifies their trajectories and changes the distribution function of the beam as it travels through the beam line. In general, this means that

the wake calculation should be done self-consistently with account of the variation of ρ and β functions caused by the wake itself. However, in many cases the effect of the beam self-field is relatively small and can be taken into account as a perturbation: the particle trajectories and the beam charge and current densities are first calculated without the account of the beam fields and used for calculation of \mathcal{W} . After \mathcal{W} is computed, one can find corrections to the original trajectories and the modification of the beam distribution function caused by the wake. As a first step in this approach, in this section, we will show how to calculate the functions $\rho(\mathbf{r}, t)$ and $\mathbf{v}(\mathbf{r}, t)$ in a beam line with a linear lattice assuming a given Gaussian distribution function of the beam at the beginning of the line. We will use the technique developed in Ref. [30] and, as already was mentioned, limit our analysis to two dimensions—the horizontal and longitudinal ones.

We use the following notations: x for the horizontal particle offset relative to the nominal orbit, $\theta = dx/ds$ for the angular slope of the orbit, $\eta = \Delta E/E$ for the relative energy deviation of the particle, z for the longitudinal coordinate of the particle in the bunch relative to the reference particle, and s for the path length along the nominal orbit. The beam distribution function $F(x, \theta, z, \eta, s)$ is a function of integrals of motion (see, e.g., [31]); it is normalized by $\int F dx d\theta dz d\eta = N_b$ where N_b is the number of particles in the bunch. We will assume that F depends on the following three integrals of motions. The first one is the action variable for the betatron oscillations in the horizontal plane,

$$J = \frac{1}{2} \frac{\alpha^2 + 1}{\beta_f} (x - D\eta)^2 + \frac{1}{2} \beta_f (\theta - D'\eta)^2 + \alpha(x - D\eta)(\theta - D'\eta), \quad (12)$$

where $\beta_f(s)$ is the beta function (not to confuse with the vector $\beta = \mathbf{v}/c$ and its components β_x and β_s below), $\alpha(s) = -\frac{1}{2} d\beta_f/ds$, $D(s)$ is the horizontal dispersion and $D'(s) = dD/ds$. The second integral of motion is the energy deviation η , which remains constant because we assume that the beam is not accelerated in the beam line and ignore the change of η caused by the CSR wake. Finally, the third integral is obtained if one expresses the initial value of the coordinate z at the beginning of the beam line (at $s = 0$) though the values of z , η , x and θ on the orbit using the transport matrix $\mathbf{R}(s)$ [30,32]. Since this initial value is a constant, the resulting expression, which we denote by Z , is an integral of motion. Using the symplecticity of the matrix \mathbf{R} , Z can be written as (see the derivation in Appendix A)

$$Z = z - R_{56}(s)\eta + xR_{26}(s) - \theta R_{16}(s). \quad (13)$$

By construction, $R_{ij}(s)$ with $i \neq j$ are equal to zero at $s = 0$, where the coordinate Z is equal to the longitudinal coordinate z in the beam.

We assume a Gaussian distribution function F ,

$$F = \frac{N_b}{2\pi\epsilon} \frac{1}{2\pi\sigma_\eta\sigma_{z0}} \exp\left(-\frac{J}{\epsilon} - \frac{(\eta - hZ)^2}{2\sigma_\eta^2} - \frac{Z^2}{2\sigma_{z0}^2}\right), \quad (14)$$

where ϵ is the horizontal emittance, σ_{z0} is the rms bunch length of the beam at $s = 0$ and σ_η is the uncorrelated energy spread of the beam. The chirp parameter h in this equation accounts for a possible correlation between the position of the particle in the bunch and its energy. This energy chirp in combination with the R_{56} element of the transport matrix is responsible for the longitudinal compression of the bunch as it travels through the beam line.

By integrating F over θ and η we can find the two-dimensional charge density of the beam along the reference orbit,

$$\rho(x, z, s) = e \int F d\theta d\eta, \quad (15)$$

and its transverse velocity

$$\beta_x(x, z, s) = \frac{e}{\rho(x, z, s)} \int F \theta d\theta d\eta, \quad (16)$$

where for a relativistic beam we used the approximation $v_x \approx c\theta$ for the horizontal component of the velocity. Substituting Eqs. (12) and (13) into Eq. (14) one can carry out the integrations in Eqs. (15) and (16) analytically. The result of the integration obtained with the symbolic integrator in *Mathematica* [33] is given by the following equations:

$$\rho(x, z, s) = \frac{eN_b}{2\pi\Sigma} \exp\left(-\frac{Ax^2 + Bxz + Cz^2}{2\beta_f\Sigma^2}\right),$$

$$\beta_x(x, z, s) = \frac{Ex + Fz}{\beta_f\Sigma^2}, \quad (17)$$

where the functions $A(s)$, $B(s)$, $C(s)$, $E(s)$, $F(s)$, and $\Sigma(s)$ are,¹

¹The expressions for these functions given in [26] are incomplete.

$$\begin{aligned}
 A &= (\alpha^2 + 1)D^2\epsilon + 2\alpha\beta_f DD'\epsilon + \beta_f[\beta_f D'^2\epsilon + \sigma_{z0}^2(hR_{56} + 1)^2 + R_{56}^2\sigma_\eta^2], \\
 B &= -2\beta_f\{D[-\alpha\epsilon + h\sigma_{z0}^2(hR_{56} + 1) + R_{56}\sigma_\eta^2] - \beta_f D'\epsilon\}, \\
 C &= \beta_f[\beta_f\epsilon + D^2(h^2\sigma_{z0}^2 + \sigma_\eta^2)], \\
 E &= (\alpha^2 + 1)D^3 D'\epsilon(h^2\sigma_{z0}^2 + \sigma_\eta^2) - D^2\epsilon\{h\sigma_{z0}^2[(\alpha^2 + 1)(hR_{56} + 1) - 2\alpha\beta_f D'^2h] + \sigma_\eta^2(-2\alpha\beta_f D'^2 + \alpha^2 R_{56} + R_{56})\} \\
 &\quad + \beta_f DD'[\beta_f D'^2\epsilon(h^2\sigma_{z0}^2 + \sigma_\eta^2) + \sigma_\eta^2\sigma_{z0}^2 + \epsilon^2] + \beta_f\epsilon[R_{56}\sigma_\eta^2(\beta_f D'^2 - \alpha R_{56}) - \sigma_{z0}^2(hR_{56} + 1)(\alpha - \beta_f D'^2h + ahR_{56})], \\
 F &= \sigma_\eta^2\epsilon[(\alpha^2 + 1)D^3 + \alpha\beta_f D(DD' + R_{56}) + \beta_f^2 D'(DD' + R_{56})] + \beta_f\epsilon(hR_{56} + 1)(h\sigma_{z0}^2(\alpha D + \beta_f D') + D\epsilon), \quad (18)
 \end{aligned}$$

and

$$\begin{aligned}
 \beta_f \Sigma^2 &= \beta_f D^2(\epsilon^2 + \sigma_\eta^2 \sigma_{z0}^2) + \epsilon \sigma_{z0}^2 [(\alpha^2 + 1)D^4 h^2 + 2\alpha\beta_f D^2 h(DD'h + hR_{56} + 1) + \beta_f^2 (DD'h + hR_{56} + 1)^2] \\
 &\quad + \sigma_\eta^2 \epsilon ((\alpha^2 + 1)D^4 + 2\alpha\beta_f D^2 (DD' + R_{56}) + \beta_f^2 (DD' + R_{56})^2). \quad (19)
 \end{aligned}$$

In these calculations we assumed zero dispersion and its derivative at the starting point, $D(0) = D'(0) = 0$. In Eqs. (17) we need to substitute $z = s - ct$; this makes ρ and β_x functions of x , s and time t and they can be used for calculations of the integrals in Eqs. (11). For the ease of notation, in what follows we will rewrite Eqs. (17) as

$$\rho(x, s, t) = n(s)e^{-a(s)x^2 - b(s)x(s-ct) - d(s)(s-ct)^2}, \quad (20a)$$

$$\beta_x(x, s, t) = e(s)x + f(s)(s - ct), \quad (20b)$$

where $a = A/2\beta_f \Sigma^2$, $b = B/2\beta_f \Sigma^2$, $d = C/2\beta_f \Sigma^2$, $n = qN_b/2\pi\Sigma$, $e = E/\beta_f \Sigma^2$ and $f = F/\beta_f \Sigma^2$. Here q denotes the particles charge.

In application of these formulas, we found a useful consistency test which helps to verify the correctness of numerical calculations. In this test, Eqs. (20) are substituted into the continuity equation $\partial_t \rho + \nabla \cdot (\rho \mathbf{v}) = 0$ and the coefficients in front of x^2 , xz , z^2 and the term that does not contain these variables are equated to zero. It is derived in Appendix B and consists of four equations (B8) to which the functions a , b , d , n , e , and f should satisfy.

IV. CALCULATION OF 2D INTEGRALS

In this section, we will show how to carry out the integration in Eqs. (11) in 2D in curvilinear coordinate system x , s associated with a plane reference orbit of the beam. This is a standard accelerator coordinate system defined by the equation

$$\mathbf{r}(s) = \mathbf{r}_0(s) + \mathbf{n}(s)x, \quad (21)$$

where $\mathbf{r}_0(s)$ is the reference orbit, $\mathbf{n}(s)$ is the normal vector and s is the arc length. The unit vector $\mathbf{n}(s)$ in combination with the tangent vector $\boldsymbol{\tau}(s) = d\mathbf{r}_0(s)/ds$ provide the basis vectors for the local coordinate system; they are continuous functions of s . They satisfy the Frenet-Serret equations,

$$\frac{d\boldsymbol{\tau}}{ds} = \frac{\mathbf{n}}{R}, \quad \frac{d\mathbf{n}}{ds} = -\frac{\boldsymbol{\tau}}{R}, \quad (22)$$

where $R(s)$ is the radius of curvature (defined by $R^{-1} = \mathbf{n} \cdot d\boldsymbol{\tau}/ds$). In this coordinate system, for the difference $|\mathbf{r}' - \mathbf{r}|$ we have

$$|\mathbf{r}' - \mathbf{r}| = |\mathbf{r}_0(s') + \mathbf{n}(s')x' - \mathbf{r}_0(s) - \mathbf{n}(s)x|. \quad (23)$$

The 2D integration is carried out using the rule

$$\int d^2 r' \rightarrow \int dx' ds' \left(1 - \frac{x'}{R(s')}\right), \quad (24)$$

where the factor $1 - x'/R$ is the Lamé coefficient that takes into account the curvilinear nature of the coordinate system (the minus sign in this coefficient corresponds to a specific choice of the direction of vector \mathbf{n} —flipping the direction of \mathbf{n} changes this sign from minus to plus).

We will use an approximation in which the transverse component β_x is assumed small, of the first order. Neglecting terms of the second order and higher, for the tangential component of the normalized velocity we have $\beta_s \approx 1$, and the velocity vector $\boldsymbol{\beta}$,

$$\boldsymbol{\beta}(x, s, t) = \boldsymbol{\tau}(s) + \mathbf{n}(s)\beta_x(x, s, t). \quad (25)$$

Using abbreviated notations: $\boldsymbol{\beta}(\mathbf{r}', t_{\text{ret}}) = \boldsymbol{\beta}'$, $\boldsymbol{\tau}(s') = \boldsymbol{\tau}'$, $\mathbf{n}(s') = \mathbf{n}'$, $\beta_x(x, s, t) = \beta_x$, and $\beta_x(x', s', t_{\text{ret}}) = \beta'_x$, we write the expression in the square brackets of Eq. (11a) as

$$\begin{aligned}
 &\boldsymbol{\beta} - (\boldsymbol{\beta} \cdot \boldsymbol{\beta}')\boldsymbol{\beta}' \\
 &= (\boldsymbol{\tau} + \mathbf{n}\beta_x) - [(\boldsymbol{\tau} + \mathbf{n}\beta_x) \cdot (\boldsymbol{\tau}' + \mathbf{n}'\beta'_x)](\boldsymbol{\tau}' + \mathbf{n}'\beta'_x) \\
 &= \boldsymbol{\tau} - (\boldsymbol{\tau} \cdot \boldsymbol{\tau}')\boldsymbol{\tau}' + \mathbf{n}\beta_x - \beta_x(\mathbf{n} \cdot \boldsymbol{\tau}')\boldsymbol{\tau}' - \beta'_x(\boldsymbol{\tau} \cdot \mathbf{n}')\boldsymbol{\tau}' - \beta'_x(\boldsymbol{\tau} \cdot \boldsymbol{\tau}')\mathbf{n}', \quad (26)
 \end{aligned}$$

where we have neglected terms of the order of $\sim \beta_x^2$ and higher. Using the relations $\boldsymbol{\tau} - (\boldsymbol{\tau} \cdot \boldsymbol{\tau}')\boldsymbol{\tau}' = (\mathbf{n}' \cdot \boldsymbol{\tau})\mathbf{n}'$ and $\mathbf{n} - (\mathbf{n} \cdot \boldsymbol{\tau}') = (\mathbf{n} \cdot \mathbf{n}')\mathbf{n}' = (\boldsymbol{\tau} \cdot \boldsymbol{\tau}')\mathbf{n}'$, we obtain

$$\boldsymbol{\beta} - (\boldsymbol{\beta} \cdot \boldsymbol{\beta}')\boldsymbol{\beta}' = (\mathbf{n}' \cdot \boldsymbol{\tau})\mathbf{n}' + (\beta_x - \beta'_x)(\boldsymbol{\tau} \cdot \boldsymbol{\tau}')\mathbf{n}' - \beta'_x(\boldsymbol{\tau} \cdot \mathbf{n}')\boldsymbol{\tau}'. \quad (27)$$

When we multiply this expression by $\partial_{r'}\rho(\mathbf{r}', t_{\text{ret}})$ in Eq. (11a) the product contains two partial derivatives of ρ ,

$$\begin{aligned} \boldsymbol{\tau}' \cdot \partial_{r'}\rho(\mathbf{r}', t_{\text{ret}}) &= \frac{1}{1 - x'/R(s')} \partial_{s'}\rho(\mathbf{r}', t_{\text{ret}}), \\ \mathbf{n}' \cdot \partial_{r'}\rho(\mathbf{r}', t_{\text{ret}}) &= \partial_{x'}\rho(\mathbf{r}', t_{\text{ret}}), \end{aligned} \quad (28)$$

where the factor $[1 - x'/R(s')]^{-1}$ in the first equation is due to the curvilinear coordinate system x, s . As a result, the integral (11a) becomes

$$\begin{aligned} \mathcal{W}_1(\mathbf{r}, t) &= -c \int \frac{dx' ds' [1 - x'/R(s')]}{|\mathbf{r}' - \mathbf{r}|} \\ &\times \left\{ [\mathbf{n}' \cdot \boldsymbol{\tau} + (\beta_x - \beta'_x)(\boldsymbol{\tau} \cdot \boldsymbol{\tau}')] \partial_{x'}\rho(\mathbf{r}', t_{\text{ret}}) \right. \\ &\left. - \frac{\beta'_x(\boldsymbol{\tau} \cdot \mathbf{n}')}{1 - x'/R(s')} \partial_{s'}\rho(\mathbf{r}', t_{\text{ret}}) \right\}. \end{aligned} \quad (29)$$

This integral does not have a singularity at $\mathbf{r}' \rightarrow \mathbf{r}$. The two partial derivatives in Eq. (29) are found from Eq. (20a):

$$\partial_{x'}\rho(x', s', t_{\text{ret}}) = [-2a(s')x' - b(s')(s' - ct_{\text{ret}})]\rho(x', s', t_{\text{ret}}), \quad (30)$$

and

$$\begin{aligned} \partial_{s'}\rho(x', s', t_{\text{ret}}) &= [-b(s')x' - 2c(s')(s' - ct_{\text{ret}})]\rho(x', s', t_{\text{ret}}) \\ &+ \left(\frac{1}{n(s')} \frac{dn(s')}{ds'} - \frac{da(s')}{ds'} x'^2 \right. \\ &\left. - \frac{db(s')}{ds'} x'(s' - ct_{\text{ret}}) - \frac{dc(s')}{ds'} (s' - ct_{\text{ret}})^2 \right) \\ &\times \rho(x', s', t_{\text{ret}}). \end{aligned} \quad (31)$$

For the second term, \mathcal{W}_2 in Eq. (11b), we need the divergence of $\boldsymbol{\beta}$, which is computed with the help of Eq. (25),

$$\begin{aligned} \partial_{r'} \cdot \boldsymbol{\beta}(\mathbf{r}', t_{\text{ret}}) &= \frac{1}{1 - x'/R(s')} \frac{\partial}{\partial x'} [1 - x'/R(s')] \beta'_x \\ &\approx \frac{e(s')}{1 - x'/R(s')}, \end{aligned} \quad (32)$$

and

$$\begin{aligned} \boldsymbol{\beta}(\mathbf{r}, t) \cdot \boldsymbol{\beta}(\mathbf{r}', t_{\text{ret}}) &= \boldsymbol{\beta} \cdot \boldsymbol{\beta}' = \boldsymbol{\tau} \cdot \boldsymbol{\tau}' + \beta_x(\mathbf{n} \cdot \boldsymbol{\tau}') + \beta'_x(\boldsymbol{\tau} \cdot \mathbf{n}') \\ &= \boldsymbol{\tau} \cdot \boldsymbol{\tau}' + (\beta_x - \beta'_x)(\mathbf{n} \cdot \boldsymbol{\tau}'), \end{aligned} \quad (33)$$

where we have used $\mathbf{n} \cdot \boldsymbol{\tau}' = -\boldsymbol{\tau} \cdot \mathbf{n}'$. With these formulas, we obtain the following expression for \mathcal{W}_2

$$\mathcal{W}_2(\mathbf{r}, t) = c \int \frac{ds' dx' e(s')}{|\mathbf{r}' - \mathbf{r}|} \boldsymbol{\tau} \cdot \boldsymbol{\tau}' \rho(x', s', t_{\text{ret}}), \quad (34)$$

where we have neglected higher order terms $\sim \beta_x^2$. Note that the integrand has an integrable singularity when $\mathbf{r} \rightarrow \mathbf{r}'$.

Finally, to calculate \mathcal{W}_3 , we need

$$\partial_{t_{\text{ret}}} \boldsymbol{\beta}(\mathbf{r}', t_{\text{ret}}) = -cf(s')\mathbf{n}'. \quad (35)$$

This gives the following expression,

$$\mathcal{W}_3(\mathbf{r}, t) = c \int \frac{ds' dx' (1 - x'/R(s')) f(s')}{|\mathbf{r}' - \mathbf{r}|} \boldsymbol{\tau} \cdot \mathbf{n}' \rho(x', s', t_{\text{ret}}), \quad (36)$$

where we again neglected terms $\sim \beta_x^2$. This integral does not have a singularity at $\mathbf{r} \rightarrow \mathbf{r}'$.

V. NUMERICAL EXAMPLE

Here we will illustrate the technique developed in the previous sections by calculating the CSR wake for a beam with an energy chirp passing through a bending magnet. Previously [26,27] we have shown that our method reproduces the transient wake in a bend of finite length in excellent agreement with 1D model [4,5] when the energy chirp in the beam is neglected. The energy chirp introduces two additional elements to the problem. First, due to the horizontal dispersion in the bend the beam spreads out in the transverse direction eventually deviating from the approximation of the 1D model. Second, the bunch length varies along the beam path—the effect that is not accurately treated in 1D.² To focus on only these two effects we calculate the wake far enough from the entrance to the bend, so that the effects associated with the entrance are ignored.

The parameters of the calculations are the following: at $s = 0$ the beam enters into uniform magnetic field and travels on a circular orbit with the bending radius $R = 1$ m. The initial beta function in the horizontal plane, $\beta_f(0) = 8$ m and has zero derivative, $\alpha(0) = 0$. The beam has the following parameters: the horizontal emittance $\epsilon = 5$ nm, the rms relative energy spread $\sigma_\eta = 10^{-4}$, the initial rms bunch length $\sigma_{z,0} = 1$ mm, the energy chirp $h = 0.01$ mm⁻¹. These parameters correspond to the initial rms transverse size $\sigma_{x,0} = 0.2$ mm. The plot of functions

²Strictly speaking, in the derivation of the 1D CSR wake [4,5], the bunch length is assumed constant. In practical applications, this requirement is usually ignored when one uses the local bunch length on the orbit.

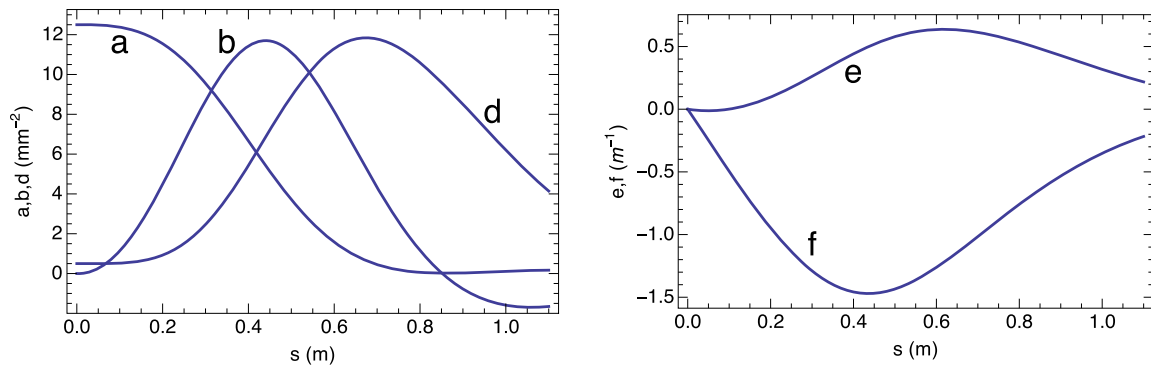


FIG. 1. Plot of the functions $a(s)$, $b(s)$, $d(s)$ (left panel) and $e(s)$, $f(s)$ (right panel). Note that the first three functions have dimension of the inverse length squared and are measured in mm^{-2} , while the last two have the dimension of the inverse length and are measured in m^{-1} . The arc length s is measured from the entrance to the magnet.

$a(s)$, $b(s)$, $d(s)$, $e(s)$ and $f(s)$ defined in Eqs. (20) for this case is shown in Fig. 1.

As the beam travels on a circular orbit its rms dimensions change. The plots of $\sigma_z(s)$ and $\sigma_x(s)$ are shown in Fig. 2. The length σ_z reaches the minimum value of 0.01 mm at $s = s_* = 0.85$ m and starts to increase at $s > s_*$ where the beam enters into an “overcompression” mode, with the particles that were initially at the head of the bunch shifted toward the tail.

As is well known, the distribution function (20a) has elliptic isolines in the plane $x - z$. The major axis of such an ellipse is initially directed along the z -axis. Inside the magnet, due to the combination of the energy chirp and dispersion, the tilt angle ξ of this ellipse (this angle is initially equal to zero) rotates in the $x-z$ plane. As a function of s this angle is defined by the following equation,

$$\tan \xi = \frac{a - d - \sqrt{(a - d)^2 + b^2}}{b}. \quad (37)$$

The angle ξ reaches the value $\pi/2$ at the point of the minimum bunch length, $s = s_*$, where $\tan \xi = \infty$. In our

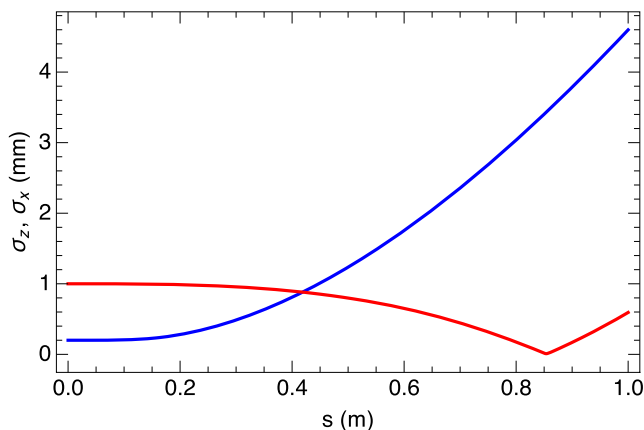


FIG. 2. Plot of the rms longitudinal (red) and horizontal (blue) bunch lengths as functions of arc length s .

calculations we compute the wake on the major axis of the beam, that is along the line $x = z \tan \xi$ (we remind the reader that the positive values of z correspond to the head of the bunch).

Using equations derived in Sec. IV we calculated the CSR wake at three different locations in the magnet, $s = 0.6$, 0.8 and 0.99 m. Note that the last value of s corresponds to the over-compressed bunch. The plots of the wakefields are shown in Fig. 3 together with the steady-state 1D wake that uses the local value of σ_z . We also calculated the wake with the computer code CSRTRACK using 50 thousand macroparticles—they are shown in Fig. 3 by green dots.³ One can see that our 2D results agree reasonably well with the 3D option of the CSRTRACK, even though the latter shows much noise due to the discreteness of macroparticles. At the same time, the 1D model strongly deviates from both the 2D and 3D wakes, which is not surprising because the beam at these locations has a relatively large tilt and a rapidly varying bunch length—the features that are not properly treated in 1D.

To illustrate the contribution of the three different parts of the wake \mathcal{W} , in Fig. 4 we plot the functions $\mathcal{W}_1(z)$, $\mathcal{W}_2(z)$ and $\mathcal{W}_3(z)$ defined by Eqs. (29), (34), and (36), respectively, for $s = 0.99$ m. One can see from this plot that while the last term, $\mathcal{W}_3(z)$, is relatively small, the other two are comparable to each other. From Eq. (11) it follows that $\mathcal{W}_2(z)$ is defined by the divergence of the velocity distribution inside the bunch that is responsible for compression (or decompression) of the bunch charge distribution. At the other two locations shown in Fig. 3, $s = 0.6$ m and (c) $s = 0.8$ m, the relative magnitude of $\mathcal{W}_1(z)$, $\mathcal{W}_2(z)$ and $\mathcal{W}_3(z)$ is qualitatively the same: $\mathcal{W}_3(z)$ is much smaller than $\mathcal{W}_1(z)$, $\mathcal{W}_2(z)$, which are about of the same magnitude and of opposite sign.

³CSRTRACK uses an adaptive time step which does not allow to output the wake at arbitrary values of s . In Fig. 2 we show the CSRTRACK wakes at positions nearest to the values indicated in the plots.

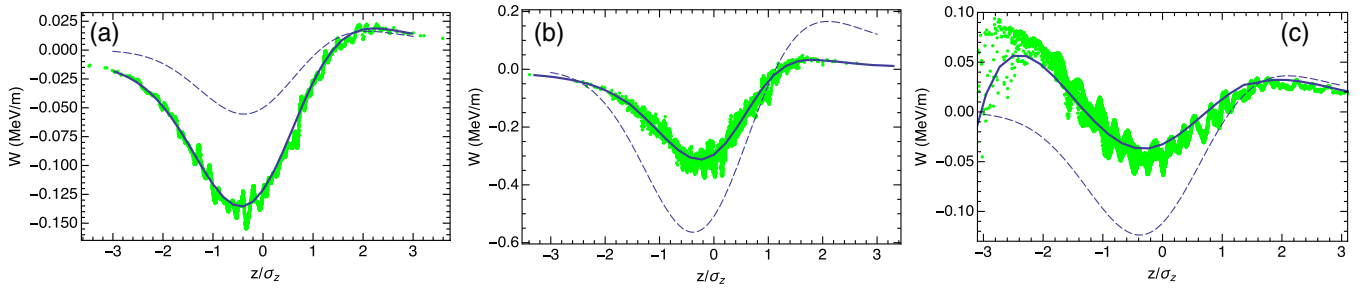


FIG. 3. Plots of the CSR wake along the semi major-axis of the beam, $x = z \tan \xi$, at three locations, (a) $s = 0.6$ m, (b) $s = 0.8$ m and (c) $s = 0.99$ m, shown by solid lines; for comparison also shown by dashed lines is the CSR wake calculated using the 1D CSR model with a local value of σ_z . The green dots show the CSR wakefield calculated with CSRTRACK. In each case the longitudinal coordinate z is normalized to the local value of σ_z .

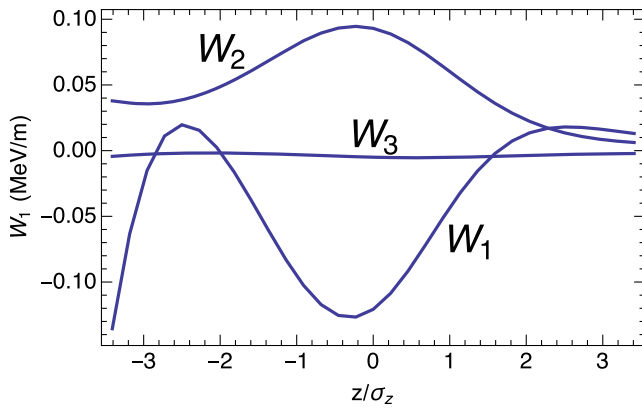


FIG. 4. Plot the functions $W_1(z)$, $W_2(z)$, and $W_3(z)$ for $s = 0.99$ m. The sum of these functions gives the solid line in Fig. 3(c).

To conclude this section, we note that calculations of the CSR wake with our method turned out to be from 6 to 30 times faster than with CSRTRACK. Our algorithm was implemented as a MATLAB script, and we expect that its

speed can be further improved when it is implemented as a stand-alone code in one of modern computer languages.

VI. BERLIN BENCHMARK CHICANE

To illustrate how our model can be used on general linear lattice, we calculated the CSR wake in a four-dipole chicane compressor studied at the CSR workshop at DESY-Zeuthen in 2002 [34]. The four magnets have the length $L = 0.5$ m with the bending radius $R = 10.35$ m resulting in the momentum compaction factor $R_{56} = 2.5$ cm. We chose a similar set of beam parameters: 5.0 GeV nominal energy, 1 nC charge, 10^{-4} initial slice energy spread and $200 \mu\text{m}$ initial rms length. The energy chirp of the beam is tuned from 36 m^{-1} to 40 m^{-1} to achieve the final bunch length ranging from $20 \mu\text{m}$ to $2 \mu\text{m}$, corresponding to final peak current ranging from 6 kA to 36 kA.

The CSR wake calculated by 1D and 2D models inside different magnets of the chicane is shown in Fig. 5. The 2D wakes plotted are actually calculated along the axis of the tilted beam. In all three cases, our method shows good agreement with CSRTRACK. In the second and third magnet

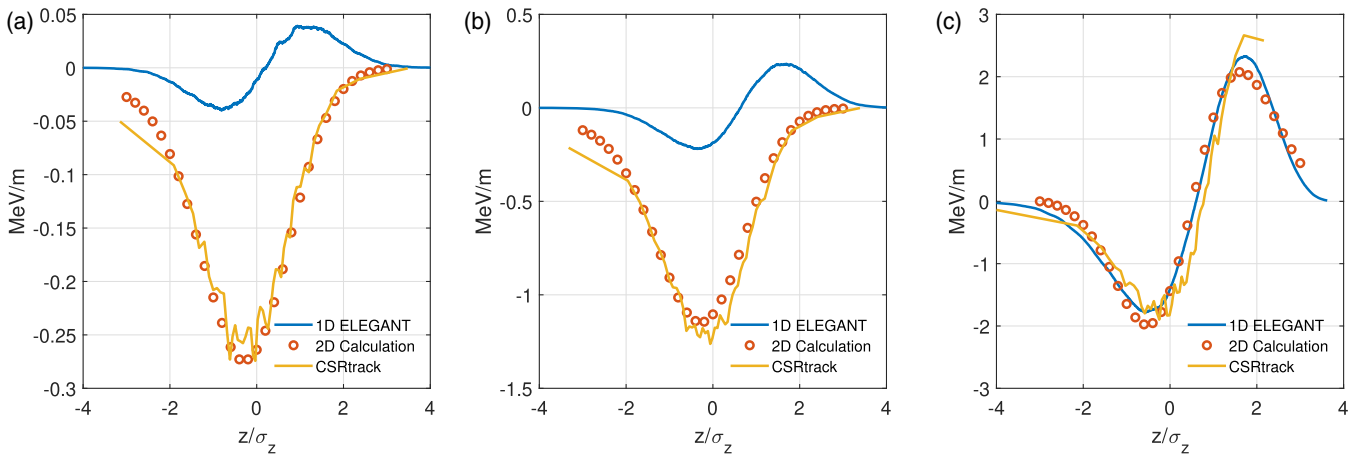


FIG. 5. Wakes calculated in 1D model are shown by blue lines and ones calculated in our 2D model and CSRTRACK are shown by circles and yellow lines respectively: (a) in the middle of the second magnet, (b) in the middle of the third magnet, and (c) in the middle of the fourth magnet. The coordinate z is normalized by the rms bunch length, $\sigma_z(s)$, at the location of the bunch.

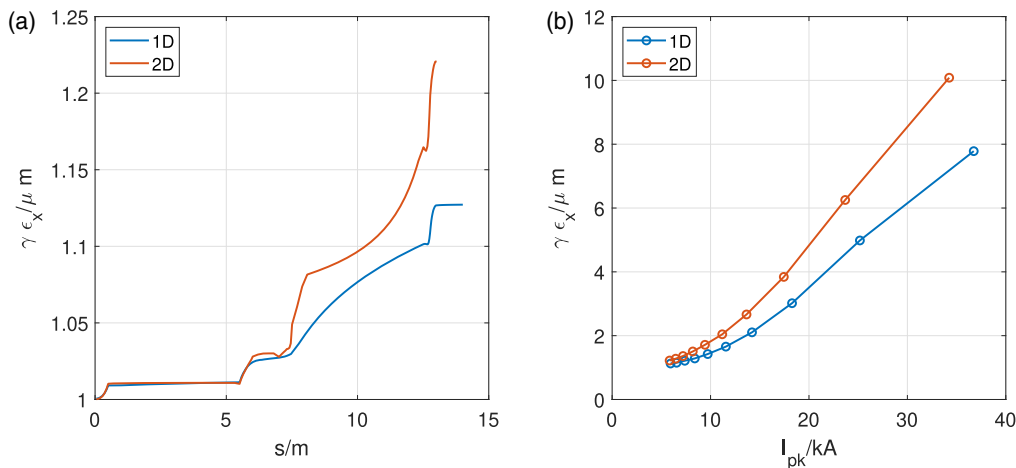


FIG. 6. Comparison of emittance growth calculated by 1D and 2D models. (a) Normalized emittance growth inside the chicane as a function of longitudinal coordinates s , with energy chirp $h = 36 \text{ m}^{-1}$. Dispersion is subtracted with second order polynomial fitting. (b) Final emittance at the end of the chicane as a function of final peak current.

[Fig. 5(a) and (b)], 2D models show large deviation from 1D model due to the beam tilt in x - z plane and therefore the transverse size of the bunch becomes much larger than the longitudinal one. As a comparison, in the last magnet the results from 1D and 2D methods converge as the tilt vanishes.

The emittance growth and other statistical properties of the beam can be simulated in our approach in a perturbative way. In the first step we divide the whole chicane into multiple slices, with more slicing in the magnets and less slicing in the drifts. At each slice we calculate the CSR induced energy loss rate in x - z plane, for which the 2D mesh is defined to cover the tilted beam. In the second step we launch macroparticles with Gaussian distribution and the same initial beam parameters, propagating it along the chicane by its transfer matrix. At each slice, we modify the energy of each macroparticle by 2D interpolation of the energy loss in x - z plane calculated in the first step. The emittance is then obtained from the particles at the end of the chicane.

The comparison between the emittance from 1D and 2D model is shown in Fig. 6. As we can see in Fig. 6(b), at relatively low peak current, 1D and 2D models show consistent final emittance, since most part of the energy loss happens in the last magnets where differences between 1D and 2D models are not significant. However, for beam with final peak current over 20 kA, emittance calculated by 2D model is more than 20% larger than the results in 1D.

VII. CONCLUSIONS

In this paper, we derived equations for the longitudinal CSR wakefield in free space that reduce the calculation to 3D (or 2D) integration along the orbit of the beam. This wake includes the effects of the beam radiation, as well as the energy change caused by the transverse and longitudinal compression of the beam. We obtained

analytical expressions for the integrands for a 2D Gaussian bunch with an energy chirp propagating through an arbitrary general linear lattice. Our numerical examples of a bunch with an energy chirp moving inside a bending magnet showed a good agreement with CSRTRACK in a situation where the 1D model fails to accurately predict the wakefield. Our method can be used for quick evaluation of the CSR wakefields in bunch compressors, wigglers, and other magnetic systems if the bunch is short enough that one can neglect the shielding effects of the metal boundaries.

Our analysis in this paper was limited by the assumption of a Gaussian distribution function (14) of the beam, which allowed us to carry out some of the integrations analytically. It can be straightforwardly extended to more general distribution functions by representing them as a superposition of Gaussian ones. Another option is, of course, to compute the charge and the transverse velocity of the beam, Eqs. (15) and (16), by a direct numerical integration of the distribution function F .

ACKNOWLEDGMENTS

We would like to thank Y. Cai, C. Mayes, Z. Huang and R. Warnock for useful discussions of various aspects of this work. This work was supported by the Department of Energy, Contract No. DE-AC03-76SF00515.

APPENDIX A: DERIVATION OF EQ. (13)

We need to define a four-dimensional transport matrix $\mathbf{R}(s)$, given by

$$\mathbf{R}(s) = \begin{pmatrix} R_{11} & R_{12} & 0 & R_{16} \\ R_{21} & R_{22} & 0 & R_{26} \\ R_{51} & R_{52} & 1 & R_{56} \\ 0 & 0 & 0 & 1 \end{pmatrix}. \quad (\text{A1})$$

This matrix acts on the coordinate vector $(X, \Theta, Z, \eta)^T$, where the capital letters denote the values of the corresponding variables x, θ and z at the entrance, and propagates it from the beginning of the beam line to position s . We emphasize that $\mathbf{R}(s)$ is a *symplectic* matrix, i.e. it satisfies the equality $\mathbf{R}^T \mathbf{J} \mathbf{R} = \mathbf{J}$, with

$$\mathbf{J} = \begin{pmatrix} 0 & 1 & 0 & 0 \\ -1 & 0 & 0 & 0 \\ 0 & 0 & 0 & 1 \\ 0 & 0 & -1 & 0 \end{pmatrix}. \quad (\text{A2})$$

Using Eq. (A1), we can find that the change in the longitudinal position of a particle from the entrance to position s is given by

$$z = Z + R_{51}X + R_{52}\Theta + R_{56}\eta. \quad (\text{A3})$$

The backward transformation from position s to the entrance is given by the inverse matrix \mathbf{R}^{-1} . From the symplectic character of \mathbf{R} , we can show that $\mathbf{R}^{-1} = -\mathbf{J} \mathbf{R}^T \mathbf{J}$. Calculating \mathbf{R}^{-1} and then multiplying this matrix by $(x, \theta, z, \eta)^T$, one finds that

$$Z = z + R_{26}x - R_{16}\theta - R_{56}\eta, \quad (\text{A4})$$

which is Eq. (13).

APPENDIX B: CONTINUITY EQUATION AND CONSISTENCY TEST

The continuity equation for the beam charge density and velocity can be also written as

$$\frac{d \ln \rho}{dt} + \text{div } \mathbf{v} = 0, \quad (\text{B1})$$

For the charge density from Eq. (20a) we have

$$\ln \rho = \ln n(s) - a(s)x^2 - b(s)x(s - ct) - d(s)(s - ct)^2. \quad (\text{B2})$$

For the velocity, we use the expression $\mathbf{v} \approx c\boldsymbol{\tau} + c\beta_x \mathbf{n}$ with $\beta_x \ll 1$, and neglect higher-order terms in β_x . Using Eq. (20b) for β_x , in the lowest approximation, we find,

$$\text{div } \mathbf{v} \approx c \frac{\partial \beta_x}{\partial x} = ce(s), \quad (\text{B3})$$

and

$$\begin{aligned} \frac{d \ln \rho}{dt} &= \frac{\partial \ln \rho}{\partial t} + \mathbf{v} \cdot \nabla \ln \rho \\ &\approx \frac{\partial \ln \rho}{\partial t} + c \frac{1}{1 - x/R} \frac{\partial \ln \rho}{\partial s} + v_x \frac{\partial \ln \rho}{\partial x}. \end{aligned} \quad (\text{B4})$$

Note that calculating $\nabla \rho$ we took into account the curvature of the trajectory through the factor $(1 - x/R)^{-1} \approx 1 + x/R$. We assume that $x \ll R$ and will use this correction only with the largest term below. Using Eq. (B2), for the partial time derivative we obtain

$$\frac{\partial \ln \rho}{\partial t} = c(bx + 2dz), \quad (\text{B5})$$

with $z = s - ct$ (in this equation and in what follows we drop the argument s in all functions). For the second term on the right of Eq. (B4) we obtain

$$\begin{aligned} \left(1 + \frac{x}{R}\right) \frac{\partial \ln \rho}{\partial s} &\approx \frac{n'}{n} - a'x^2 - b'xz - d'z^2 \\ &\quad - \left(1 + \frac{x}{R}\right)bx - 2\left(1 + \frac{x}{R}\right)dz, \end{aligned} \quad (\text{B6})$$

where the prime denotes the derivative with respect to s . The last two terms in this expression are the biggest ones, so we keep the small factor x/R in front of them; for the other terms we neglected x/R . Finally, for the last term in (B4), we have

$$v_x \frac{\partial \ln \rho}{\partial x} = -c(ex + fz)(2ax + bz). \quad (\text{B7})$$

Combining everything and requiring that the resulting expression be identically equal to zero for arbitrary x and z we arrive at the following four relations:

$$\begin{aligned} \frac{n'}{n} &= -e, \\ 2ea + \frac{e}{R} &= -a', \\ fb &= -d', \\ 2fa + eb + \frac{2d}{R} &= -b'. \end{aligned} \quad (\text{B8})$$

Given the complexity of the expressions for a, b, d, e, f, n , these relations provide a useful check of numerical calculations of these functions for a given beam line.

-
- [1] J. B. Murphy, S. Krinsky, and R. L. Gluckstern, Longitudinal wakefield for synchrotron radiation, in *Proc. IEEE Particle Accelerator Conference and International Conference on High-Energy Accelerators, Dallas, 1995*

- (IEEE, Piscataway, NJ, 1996), pp. 2980–2982, (IEEE Conference Record 95CH35843).
- [2] J. B. Murphy, S. Krinsky, and R. L. Gluckstern, Longitudinal wakefield for an electron moving on a circular orbit, *Part. Accel.* **57**, 9 (1997).
 - [3] Y. S. Derbenev, J. Rossbach, E. L. Saldin, and V. D. Shiltsev, *Microbunch Radiative Tail-Head Interaction*, DESY FEL Report TESLA-FEL 95-05 (Deutsches Elektronen-Synchrotron, Hamburg, Germany, 1995).
 - [4] E. L. Saldin, E. A. Schneidmiller, and M. V. Yurkov, On the coherent radiation of an electron bunch moving in an arc of a circle, *Nucl. Instrum. Methods Phys. Res., Sect. A* **398**, 373 (1997).
 - [5] G. Stupakov and P. Emma, CSR wake for a short magnet in ultrarelativistic limit, in *Proceedings of the 8th European Particle Accelerator Conference, Paris, 2002* (EPS-IGA and CERN, Geneva, 2002), p. 1479.
 - [6] C. Mayes and G. Hoffstaetter, Exact 1D model for coherent synchrotron radiation with shielding and bunch compression, *Phys. Rev. Accel. Beams* **12**, 024401 (2009).
 - [7] D. Sagan, G. Hoffstaetter, C. Mayes, and U. Sae-Ueng, Extended one-dimensional method for coherent synchrotron radiation including shielding, *Phys. Rev. Accel. Beams* **12**, 040703 (2009).
 - [8] W. Lou and G. H. Hoffstaetter, Coherent synchrotron radiation wake expressions with two bending magnets and simulation results for a multiturn energy-recovery linac, *Phys. Rev. Accel. Beams* **23**, 054404 (2020).
 - [9] A. Brynes, P. Smorenburg, I. Akkermans, E. Allaria, L. Badano, S. Brussaard, M. Danailov, A. Demidovich, D. N. Giovanni, D. Gauthier, G. Gaio, B. van der Geer, L. Giannessi, M. Loos, N. Mirian, G. Penco, P. Ribic, F. Rossi, I. Setija, and S. Di Mitri, Beyond the limits of 1d coherent synchrotron radiation, *New J. Phys.* **20**, 073035 (2018).
 - [10] R. L. Warnock and P. Morton, Fields excited by a beam in a smooth toroidal chamber, *Part. Accel.* **25**, 113 (1990).
 - [11] G. V. Stupakov and I. A. Kotelnikov, Shielding and synchrotron radiation in toroidal waveguide, *Phys. Rev. Accel. Beams* **6**, 034401 (2003).
 - [12] T. Agoh and K. Yokoya, Calculation of coherent synchrotron radiation using mesh, *Phys. Rev. Accel. Beams* **7**, 054403 (2004).
 - [13] G. Stupakov and I. A. Kotelnikov, Calculation of CSR impedance using mode expansion method, *Phys. Rev. Accel. Beams* **12**, 104401 (2009).
 - [14] T. Agoh, Steady fields of coherent synchrotron radiation in a rectangular pipe, *Phys. Rev. Accel. Beams* **12**, 094402 (2009).
 - [15] D. Zhou, K. Ohmi, K. Oide, L. Zang, and G. Stupakov, Calculation of coherent synchrotron radiation impedance for a beam moving in a curved trajectory, *Jpn. J. Appl. Phys.* **51**, 016401 (2012).
 - [16] G. Stupakov and D. Zhou, Analytical theory of coherent synchrotron radiation wakefield of short bunches shielded by conducting parallel plates, *Phys. Rev. Accel. Beams* **19**, 044402 (2016).
 - [17] G. Bassi, J. A. Ellison, K. Heinemann, M. Venturini, and R. Warnock, Self-consistent computation of electromagnetic fields and phase space densities for particles on curved planar orbits, in *Proceedings of the 2007 Particle Accelerator Conference* (IEEE, New York, 2007).
 - [18] G. Bassi, J. A. Ellison, K. Heinemann, and R. Warnock, Microbunching instability in a chicane: Two-dimensional mean field treatment, *Phys. Rev. Accel. Beams* **12**, 080704 (2009).
 - [19] M. Dohlus, Field calculations for bunch compressors, in *ICFA Beam Dynamics mini workshop: Coherent Synchrotron Radiation and its impact on the dynamics of high brightness electron beams* (DESY-Zeuthen, Germany, 2002).
 - [20] G. Stupakov, Synchrotron radiation wake in free space, in *Proceedings of the 1997 Particle Accelerator Conference*, Vol. 2 (IEEE, Piscataway, NJ, 1998), pp. 1688–90.
 - [21] Y. Cai, Coherent synchrotron radiation by electrons moving on circular orbits, *Phys. Rev. Accel. Beams* **20**, 064402 (2017).
 - [22] Y. Cai and Y. Ding, Three-dimensional effects of coherent synchrotron radiation by electrons in a bunch compressor, *Phys. Rev. Accel. Beams* **23**, 014402 (2020).
 - [23] M. Dohlus and T. Limberg, CSRtrack: Faster calculations of 3-D CSR effects, in *Proceedings of FEL2004 Conference* (Comitato Conferenze Elettra, Trieste, Italy, 2004), pp. 18–21.
 - [24] D. Ratner, Much ado about microbunching: Coherent bunching in high brightness electron beams, Ph.D. thesis, SLAC, 2011.
 - [25] G. Stupakov, A Novel One-Dimensional Model for CSR Wakefields, in *Proceedings, 39th International Free Electron Laser Conference, FEL2019* (JACoW Publishing, Geneva, Switzerland, 2019), p. THP037, <https://doi.org/10.18429/JACoW-FEL2019-THP037>.
 - [26] J. Tang and G. Stupakov, Fast two-dimensional calculation of coherent synchrotron radiation in relativistic beams, in *Proceedings of the 2019 North American Particle Accelerator Conference (NAPAC19)*, Lansing, Michigan (JACoW Publishing, Geneva, Switzerland, 2019), p. WEPLS09, <https://doi.org/10.18429/JACoW-NA-PAC2019-WEPLS09>.
 - [27] G. Stupakov, New Method of Calculation of the Wake due to Radiation and Space Charge Forces in Relativistic Beams, in *Proceedings, 10th International Particle Accelerator Conference: Melbourne, Australia, May 19-24, 2019* (JACoW, Geneva, 2019), p. 1223.
 - [28] L. D. Landau and E. M. Lifshitz, *The Classical Theory of Fields*, 4th ed., Course of Theoretical Physics, Vol. 2 (Pergamon, London, 1979) (Translated from Russian).
 - [29] J. D. Jackson, *Classical Electrodynamics* (Wiley, New York, 1999).
 - [30] S. Heifets, G. Stupakov, and S. Krinsky, Coherent synchrotron radiation instability in a bunch compressor, *Phys. Rev. Accel. Beams* **5**, 064401 (2002).
 - [31] G. Stupakov and G. Penn, *Classical Mechanics and Electromagnetism in Accelerator Physics*, Graduate Texts in Physics (Springer International Publishing, New York, 2018).

-
- [32] P. Baxevanis and G. Stupakov, Transverse dynamics considerations for microbunched electron cooling, *Phys. Rev. Accel. Beams* **22**, 081003 (2019).
- [33] Wolfram Research, Inc., Mathematica, Version 12.1 (2020).
- [34] P. Emma, CSR Benchmark Test-Case Results, in *ICFA Beam Dynamics mini workshop: Coherent Synchrotron Radiation and its impact on the dynamics of high brightness electron beams* (DESY-Zeuthen, Germany, 2002).